

Definition and geometrical consideration of the domain walls of  $Pb_3(PO_4)_2$  ferroelastic crystals

Se-Young Jeong and Min-Su Jang

Department of Physics, Pusan National University, Pusan 609-735, Korea

Ae-Ran Lim

Department of Physics, Jeonju University, Chonju 560-759, Korea

(Received 1 February 1993)

$Pb_3(PO_4)_2$  has two types of domain walls, the  $W$  wall and the  $W'$  wall. However, both types of domain walls in  $Pb_3(PO_4)_2$  belong to the  $W$  wall, because they both can be represented as crystallographically prominent planes of fixed indices. We will call them the  $W_m$  wall and the  $W_b$  wall instead of the  $W$  wall and the  $W'$  wall, respectively. The  $z$  axis of the prototypic phase is not parallel but a little inclined to the normal of (100). Local reorientations in a narrow temperature range near  $T_c$  cause superpositions of small inclined  $z$  axes above  $180^\circ C$ , which give a small birefringence at the conoscope image.

I. INTRODUCTION

Lead phosphate,  $Pb_3(PO_4)_2$ , is a well-known ferroelastic crystal. In our previous work,<sup>1</sup> we reported the results of the observation of domains using a polarization microscope and we also proposed some models to describe the domain walls.

It was reported that  $Pb_3(PO_4)_2$  has two types of domain walls, the  $W$  wall and the  $W'$  wall.<sup>2</sup> But we suggest here that  $Pb_3(PO_4)_2$  has no  $W'$  walls, because both domain walls can be represented as crystallographically prominent planes of fixed indices.

Joffrin *et al.*<sup>3</sup> pointed out that, even if the overall symmetry of the  $\beta$  phase is rhombohedral, its local symmetry is in fact monoclinic. Other experimental studies involving neutron diffraction,<sup>4</sup> Raman<sup>5-7</sup> and infrared spectroscopy<sup>7,8</sup> indicated the existence of an intermediate pseudo-phase with local monoclinic symmetry and rhombohedral lattice constants.

In this work, we discuss the following two problems: (1) an alternative definition of domain walls, and (2) the structural details of  $Pb_3(PO_4)_2$  above  $180^\circ C$ , which specify why, even if the overall symmetry of the  $\beta$  phase is rhombohedral, the experimental results indicate that it has local monoclinic symmetry or a small birefringence.

II. TWO TYPES OF PERMISSIBLE DOMAIN WALLS

A planar stress-free domain wall can exist only along that plane which, as a result of the ferroelastic phase transition, undergoes equal deformations in the two domains separated by the wall.<sup>9</sup> Permissible domain walls in  $Pb_3(PO_4)_2$  are of two types,  $W$  walls and  $W'$  walls. It is clear that the two walls must exist by virtue of the crystal symmetry. The  $W$  wall results from twinning by the pseudomirror planes  $(11\bar{3})$  or  $(1\bar{1}\bar{3})$ . The  $W'$  wall results from twinning by the pseudobinary axes  $[011]$  or  $[0\bar{1}\bar{1}]$ .<sup>10</sup> The two contiguous domains of  $W$  walls and  $W'$  walls can be deduced one from the other by a mirror symmetry and by a rotation of  $180^\circ$  relative to  $[011]$  or  $[0\bar{1}\bar{1}]$ , respectively. Figure 1(a) represents three orientation states with  $W'$  walls and Fig. 1(b) represents one twinning of a  $W'$  wall in the circled area of Fig. 1(a). The  $180^\circ$  rotation of  $ABabD-Ecd$  along the  $PP'$  axis reproduces  $A'B'cdD'-E'ab$ . Sapriel<sup>2</sup> used the terms  $W'$  walls for those walls for which orientation is represented by irrational indices and may only accidentally be rational. In our model  $W'$  walls are represented by rational indices but not accidentally. Since the domain wall cuts every axis in half, the  $W'$  wall is manifested by rational indices of  $(11\bar{1})$  or  $(\bar{1}11)$ .  $(111)$  and  $(1\bar{1}\bar{1})$  planes are not allowed

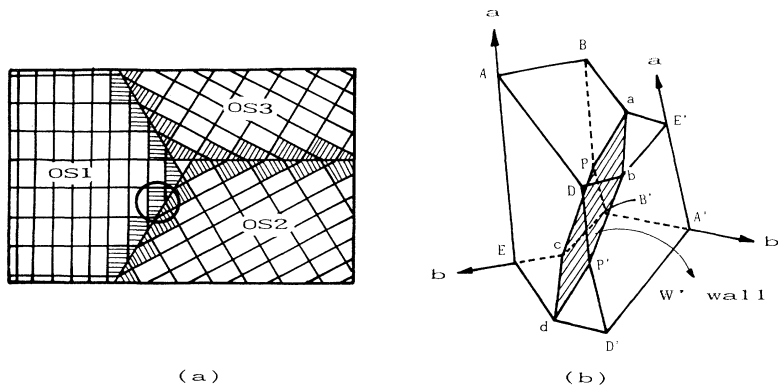


FIG. 1. (a) Schematic diagram of  $W'$  walls and three orientation states of domains. (b) Twin lattice structure at the domain boundary ( $W'$  wall).

for the  $W'$  wall, because the planes do not satisfy the symmetry of the binary axis. With this model we can induce the result that  $\text{Pb}_3(\text{PO}_4)_2$  has two types of  $W$  walls, i.e., the tilted domain wall of  $\text{Pb}_3(\text{PO}_4)_2$  is no  $W'$  wall, but a kind of  $W$  wall.

The tilted angle of the domain wall can be computed using the projection from the (100) plane. It amounts to  $14^\circ$ , which deviates by about  $3^\circ$  from the theoretically calculated value of  $17^\circ$ .<sup>2</sup> The theoretical value depends strongly on the accuracy of the measured lattice parameters. For  $\beta=102.55^\circ$  instead of  $102.39^\circ$ , it is computed to  $14^\circ$ . The accurate value of the tilted angle of the domain wall in other ferroelastic crystals may be calculated using this twin model.

The electron-diffraction pattern of Fig. 2 was taken across a  $W$  wall. From this pattern we can see that  $(11\bar{3})$ ,  $(1\bar{1}\bar{3})$ ,  $(11\bar{1})$ , and  $(\bar{1}\bar{1}1)$  planes are prominent planes. Figure 3 shows a schematic representation of an electron-diffraction pattern taken across a  $W$  wall, which gives good agreement to the spots of Fig. 2.  $(11\bar{3})$  and  $(1\bar{1}\bar{3})$  planes correspond to  $W$  walls. Torr s, Roucau, and Ayroles<sup>11</sup> also observed electron-diffraction patterns and expounded that the spots of a doublet correspond to different orientations of domains. But our results clarify that the doublet is produced not by the different orientations of domains, but because the  $(11\bar{3})$  plane and the  $(1\bar{1}\bar{1})$  plane do not intersect at exactly  $90^\circ$  but at about  $92^\circ$ . From the fact that the unsplit row of spots representing  $(11\bar{3})$  and  $(1\bar{1}\bar{3})$  makes about  $92^\circ$  (about  $88^\circ$  in reciprocal systems) to split rows representing  $(\bar{1}\bar{1}1)$  and  $(11\bar{1})$ , respectively, it is manifested that  $(\bar{1}\bar{1}1)$  and  $(11\bar{1})$  planes are from  $W'$  walls. In TEM photographs,<sup>12</sup>

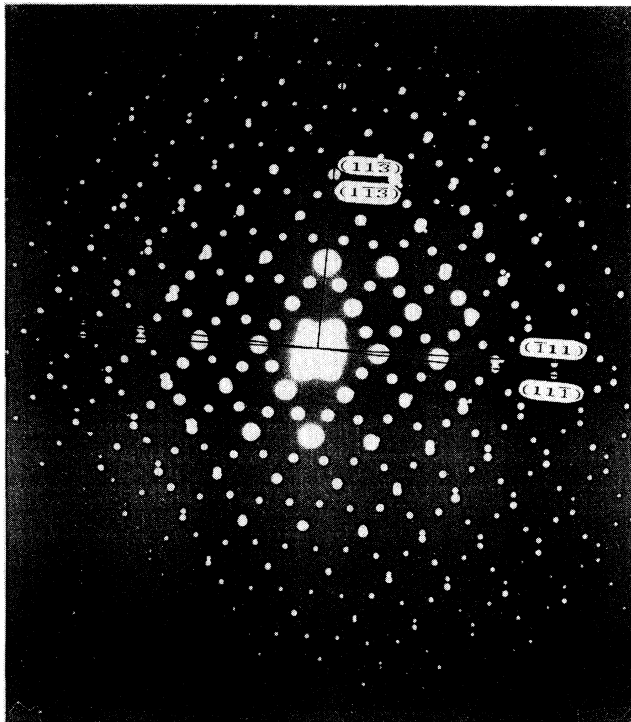


FIG. 2. Electron-diffraction pattern of  $\text{Pb}_3(\text{PO}_4)_2$ .

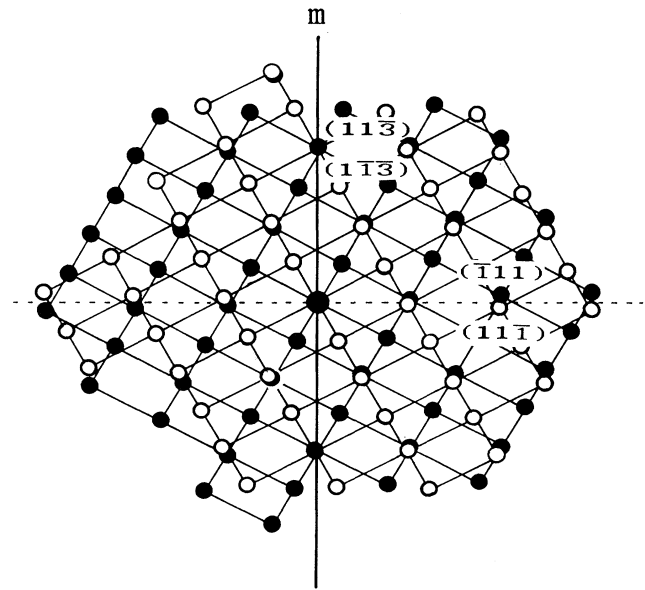


FIG. 3. Schematic representation of twin patterns taken across a  $W$  wall.

it was confirmed that the  $W$  wall makes an angle of about  $92^\circ$  to the  $W'$  wall, when the two different walls meet perpendicularly. This can be explained by using the geometrical models in Fig. 4. We conclude that  $\text{Pb}_3(\text{PO}_4)_2$  has only  $W$  walls but of two types. From now on we call the  $W$  wall and the  $W'$  wall the  $W_m$  wall and the  $W_b$  wall, respectively, where the  $W_m$  wall is the wall of twinning by the pseudomirror plane  $(11\bar{3})$  or  $(1\bar{1}\bar{3})$ ,

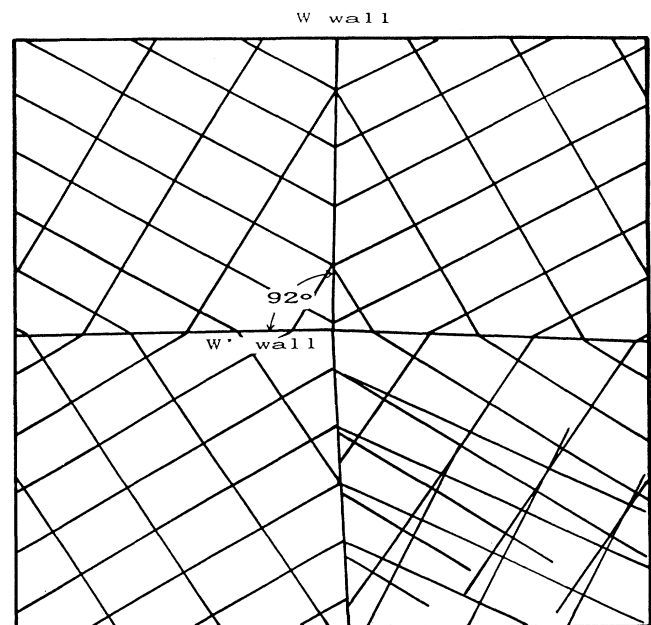


FIG. 4. Schematic representation at the intersection of two types of domain walls.

and the  $W_b$  wall is the wall of twinning by the pseudo-binary axis  $[011]$  or  $[01\bar{1}]$ . The possible indices are  $(11\bar{3})$  and  $(\bar{1}\bar{1}3)$  for the  $W_m$  wall,  $(11\bar{1})$  and  $(\bar{1}\bar{1}1)$  for the  $W_b$  wall.  $(1\bar{1}3)$ ,  $(111)$ , and  $(\bar{1}\bar{1}1)$  reflections cannot appear.

### III. THE GEOMETRY OF MONOCLINIC AND TRIGONAL STRUCTURE

Figure 5 shows how the pseudotrigonal lattice is located in monoclinic lattice.<sup>13</sup>  $ABCD-EFGH$  is one unit cell of monoclinic lattice. The direction of the line  $FK$  corresponds to the  $z$  axis of the prototypic phase. The position  $K$  halves the line  $IJ$  exactly. The direction  $FK$  makes  $13.16^\circ$  to the direction of  $FB$  and has a difference of  $0.77^\circ$  from the  $a^*$  axis [perpendicular to the  $(100)$  plane], which means that the  $z$  axis of the prototypic phase is not exactly perpendicular to the  $(100)$  plane but a little inclined.  $Pb_3(PO_4)_2$  changes its orientation easily due to external stress and shows superpositions of various twin orientation under a particular stress.<sup>13</sup> Likewise a single domain of  $Pb_3(PO_4)_2$  changes to superpositions of various orientation near  $T_c$  before the symmetry changes to rhombohedral one. At  $T_c$ , the rhombohedral  $z$  axes orient according to one of various monoclinic orientation, i.e., two  $z$  axes of the prototypic phase, based on two different monoclinic orientations are not parallel. In the investigation of the phase change near the phase transition using the polarization microscope, it is observed that new orientations always appear before the low-temperature phase undergoes the phase transition to the high-temperature phase (Fig. 6), and the new orientations results in superpositions of various orientation. Figures 7 give a view about the superposition of the possible orientations of the monoclinic structure. If the total area with the thickness  $d$  undergoes the phase transition direct to the rhombohedral lattice without the reorientation of the

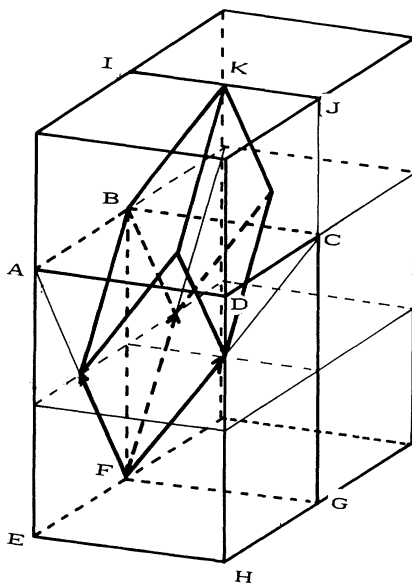


FIG. 5. The location of the pseudotrigonal lattice in monoclinic lattice.

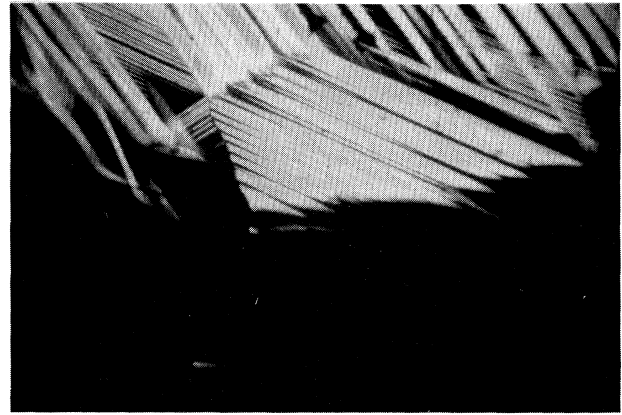


FIG. 6. The photograph taken by using the polarizing microscope about the reorientation of the monoclinic structure near transition temperature.

monoclinic structure, the inclination of  $z$  axis can be represented as in Fig. 7(b). In this case the conoscopic image of the high temperature must be a distinct uniaxial one only with a little uncentered uniaxial interference figure by the rotation of the sample. Figure 7(a) is a pro-

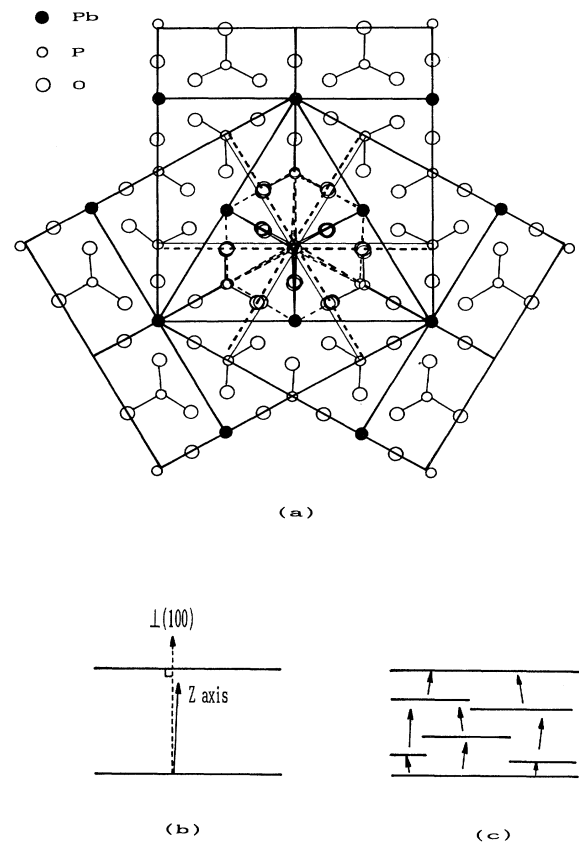


FIG. 7. (a) The projection from  $(100)$  plane in the case with the superposition of the different monoclinic orientations. (b) The direction of the  $z$  axis of the prototypic phase in the crosscut of the sample without the superposition. (c) The superposition of the direction of the  $z$  axis of the prototypic phase in the crosscut of the sample with the superposition.

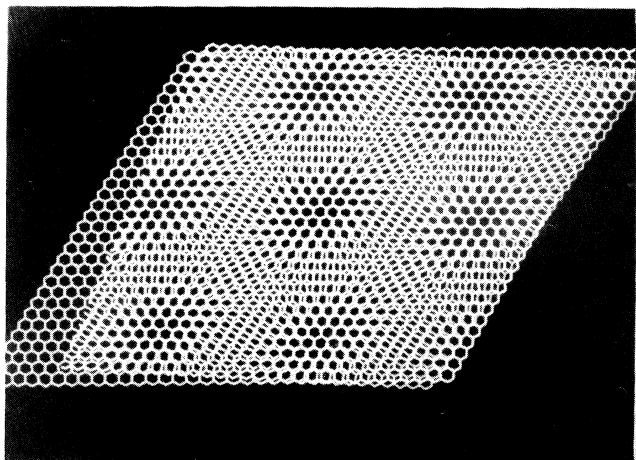


FIG. 8. Distorted hexagonal reconstruction by tilting and rotation of two graphite layers.

jection on the (100) plane supposing that a crystal plate with the thickness  $d$  was reoriented to the superposition of various monoclinic orientations. Because the rhombohedral structure above  $T_c$  is built on the basis of the reoriented monoclinic lattice, the  $z$  axis of rhombohedral phase above  $T_c$  appear as the superposition of the small inclined  $z$  axes like in Fig. 7(c). It supports the idea that the small birefringence above  $T_c$  on the observation using the polarization microscope is caused by the superposition of the inclined  $z$  axes of the prototypic phase. It is the reason that the crystal behaves as if it has small monoclinic microdomains. There were many reports<sup>3-8</sup> about the fact that small microdomains of the low-temperature phase persist, in the temperature range 180–300 °C, with three orientation variants related by a

threefold symmetry axis. We have seen in Fig. 7(a) that the  $z$  axis of the prototypic phase has three possible directions. The superpositions of three possible directions of the  $z$  axis may behave as if it has a locally multiplied monoclinic unit cell with three orientation variants.

Figure 8 is the result of the computer simulation to show the superstructure by the tilting and rotation of two graphite layers with each other.<sup>14</sup> It shows that the superpositions of two or more tilted layers with a hexagonal symmetry reconstruct the distorted superstructure.

#### IV. CONCLUSION

We made a few models of domain walls and got the result that  $W'$  walls are indexed to  $(11\bar{1})$  and  $(\bar{1}11)$ , and so  $\text{Pb}_3(\text{PO}_4)_2$  has only  $W$  walls but of two types. It was proved by the electron-diffraction pattern and by using the geometrical models. From now on we call the  $W$  and the  $W'$  wall the  $W_m$  wall and the  $W_b$  wall, respectively.

Near the phase-transition temperature new orientations always appear. Because the rhombohedral structure above  $T_c$  is built on the basis of the reoriented monoclinic lattice, the  $z$  axis of rhombohedral phase above  $T_c$  appear as the superposition of the small inclined  $z$  axes. It supports the idea that the small birefringence above  $T_c$  is caused by the superposition of the inclined  $z$  axes of the prototypic phase, which induce the multiplication of unit cells.

#### ACKNOWLEDGMENTS

We are grateful to Dr. I. S. Lee for the offering of the picture about superstructure. The present study was supported by the Korea Science and Engineering Foundation through the Science Research Center (SRC) of Excellence Program.

<sup>1</sup>S. Y. Jeong, M. S. Jang, H. J. Kim, C. R. Cho, and Y. S. Yu, *Ferroelectrics* **142**, 121 (1993).

<sup>2</sup>J. Sapriel, *Phys. Rev. B* **12**, 5128 (1975).

<sup>3</sup>C. Joffrin, J. P. Benoit, L. Deschamp, and M. Lambert, *J. Phys. (Paris)* **38**, 205 (1977).

<sup>4</sup>C. Joffrin, J. P. Benoit, R. Currat, and M. Lambert, *J. Phys. (Paris)* **40**, 1185 (1979).

<sup>5</sup>J. P. Benoit and J. P. Chapelle, *Solid State Commun.* **15**, 531 (1974).

<sup>6</sup>J. P. Benoit, *Ferroelectrics* **13**, 331 (1976).

<sup>7</sup>E. Salje and U. Bismayer, *Phase Trans.* **2**, 15 (1981).

<sup>8</sup>Y. Luspain, L. L. Servoin, and F. Gervais, *J. Phys. Chem.*

*Solids*, **40**, 661 (1979).

<sup>9</sup>J. Fousek and V. Janovec, *J. Appl. Phys.* **40**, 135 (1969).

<sup>10</sup>M. Chabin, J. P. Ildefonse, and F. Gilletta, *Ferroelectrics* **13**, 333 (1976).

<sup>11</sup>J. Torrès, C. Roucau, and R. Ayroles, *Phys. Status Solidi A* **70**, 659 (1982).

<sup>12</sup>A. R. Lim, K. H. Lee, S. H. Choh, S. Y. Jeong, and M. S. Jang, *J. Korean Phys. Soc.* **26**, 384 (1993).

<sup>13</sup>E. K. H. Salje, *Phase Transition in Ferroelastic and Co-elastic Crystals* (Cambridge University, Cambridge, England, 1990).

<sup>14</sup>I. S. Lee, Ph.D. thesis, University of Bristol, 1992.

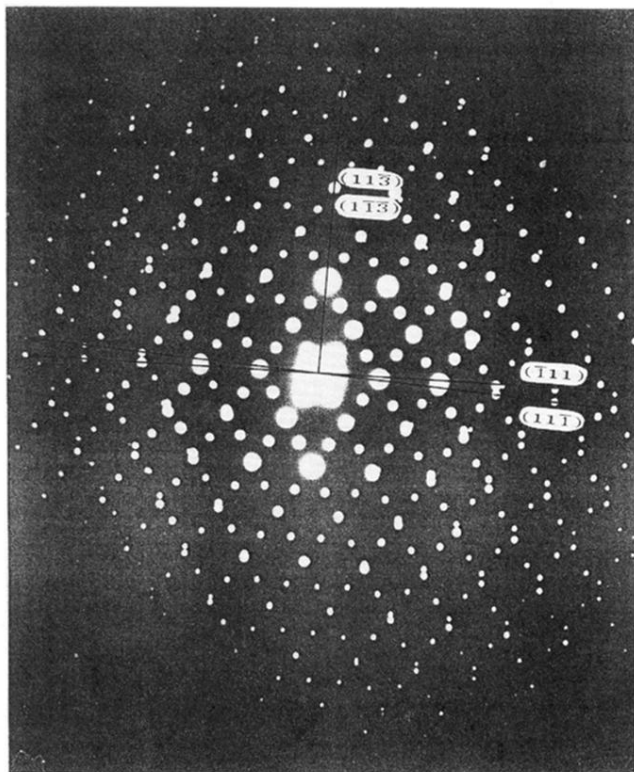


FIG. 2. Electron-diffraction pattern of  $\text{Pb}_3(\text{PO}_4)_2$ .

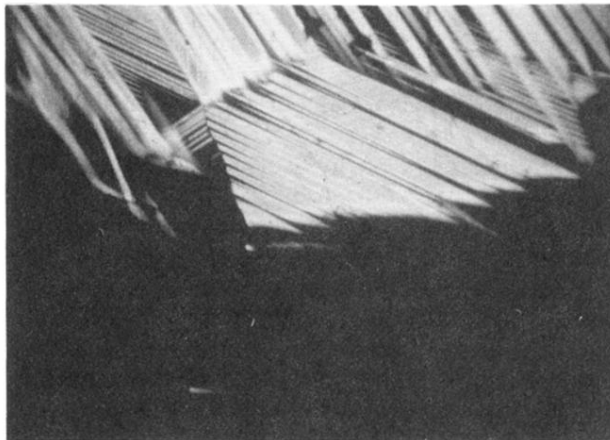


FIG. 6. The photograph taken by using the polarizing microscope about the reorientation of the monoclinic structure near transition temperature.

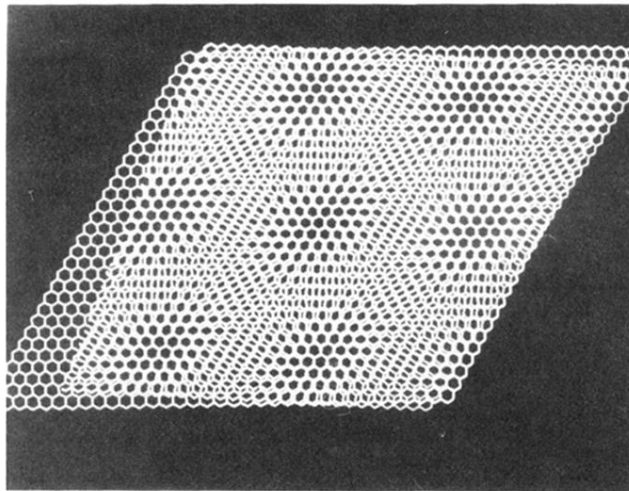


FIG. 8. Distorted hexagonal reconstruction by tilting and rotation of two graphite layers.